Surface & Coatings Technology 206 (2011) 1899–1904

Contents lists available at SciVerse ScienceDirect

Surface & Coatings Technology

journal homepage: www.elsevier.com/locate/surfcoat

Cross-linked graphene layer embedded carbon film prepared using electron irradiation in ECR plasma sputtering

Chao Wang, Dongfeng Diao *

Key Laboratory of Education Ministry for Modern Design and Rotor-Bearing System, School of Mechanical Engineering, Xi'an Jiaotong University, Xi'an 710049, China

ARTICLE INFO

Available online 3 September 2011

Keywords:
ECR plasma
Electron irradiation
Graphene layer embedded carbon
Friction mechanism

ABSTRACT

A new path to prepare cross-linked graphene layers embedded carbon (GLEC) films has been reported by introducing electron irradiation during the mirror-confinement electron cyclotron resonance (ECR) plasma sputtering process. The electron irradiation in the ECR plasma was identified by using Langmuir single probe equipped with a designed simulated substrate and the irradiation mode was found to be controlled directly by altering the substrate bias voltage. Cross-linked GLEC film was prepared using the electron irradiation in the pressure of 0.04 Pa and positive bias voltage of 50 V, and the nanostructure and binding configuration of the film were analyzed by high resolution transmission electron microscope (HRTEM) and X-ray photoelectron spectroscopy (XPS). The results showed that GLEC film contains cross-linked graphene layers grown normally to the substrate surface when the content of sp^2 hybridized carbon atoms in the film is more than 70%. The tribological behaviors of both cross-linked GLEC films and amorphous carbon films were compared using a Pin-on-Disk tribometer, and the mechanism for low friction coefficient was discussed by using HRTEM observation on wear track. The HRTEM results indicated that the cross-linked GLEC film has the potential to achieve low friction at the beginning of the friction.

1. Introduction

Carbon film with graphite like nano crystallite has drawn much interest since it has not only high hardness and good wear performances comparable to those of diamond but also wonderful electrical conductivity along basal planes which is close to that of graphite [1–3]. It has a bright future as a new coating material in modern industry. There are some researches focusing on the growing of carbon films with graphite-like nano crystallite. I. Alexandro, et al. [1] prepared nano crystallite carbon film with sp^2 network structure using laser-arc evaporation and found the film has high hardness and elastic recovery. S. Hirono, et al. [2,3] reported a carbon nano crystallite film prepared with ECR sputtering method, and studied the conductivity and the hardness of the film. However, why the film showed a nano crystallite structure was not discussed. W. M. Lau, et al. [4,5] prepared tetrahedral amorphous carbon (ta-C) film using filtered cathodic vacuum arc (FCVA) method, and studied thermally induced sp^2 clustering in the ta-C film. They found that the structure transformation through sp^2 clustering at high temperature was caused by stress relief. J. O. Orwa, et al. [6] also deposited ta-C film with different impact energy of carbon ions, and found that the structure of ta-C films can transform from amorphous into a sp^2 rich structure containing graphite layers by increasing inner stress accumulated by impacting carbon ions. However, to prepare carbon films with embedded cross-linked graphene layers using electron irradiation in ECR sputtering method has not been reported.

The outstanding tribological properties of carbon films has been realized as the low friction coefficient and long wear life, which make carbon film a class of important tribological materials [7]. Especially referring to the decreasing of friction coefficient in tribotest, as the phenomena has been observed frequently [8–11], the reason why friction coefficient decreased is still in discussion. A. Erdemir, et al. [12] researched the chemical composition and test condition as factors that influence the friction coefficient of carbon films and suggested that hydrogen connecting with surface carbon atoms is essential for carbon films to achieve low friction, and the water vapor in ambient condition also plays an important role in the low friction of hydrogen-free carbon film, as the water molecules can provide hydrogen atoms in surface sliding process. H. Ronkainen, et al. [13] studied the environmental and thermal effects on tribological properties of diamond like carbon films, and found that graphitization of the carbon film may be one cause of the friction coefficient decreasing in ambient environment. T. W. Scharf and I. L. Singer [14] examined the tribological behavior of several amorphous carbon film during the run in stage (before friction coefficient decrease), and found that the formation of a stationary transfer film is decisive for the friction coefficient decreasing. However, the above research and findings were supported by optical observations such as bright-field transmission electron microscopy (TEM) [15–17], or spectroscopy results such as Raman spectrum [10,18]. More directive and strong evidence

* Corresponding author.
E-mail address: dfdiao@mail.xjtu.edu.cn (D. Diao).

0257-8972/$ – see front matter © 2011 Elsevier B.V. All rights reserved.
doi:10.1016/j.surfcoat.2011.08.009

such as high resolution transmission electron microscopy (HRTEM) observation on the atom-level structural change details of the carbon film in tribological actions has not been reported yet.

In this study, a new path to prepare cross-linked graphene layers embedded carbon (GLEC) film by inducing electron irradiation in ECR plasma sputtering method was reported, the nanostructure of the GLEC film was studied by HRTEM, and the mechanism of low friction in tribological test of the film was discussed by HRTEM observation on the wear track.

2. Experimental details

2.1. Plasma diagnosis

The plasma diagnosis was carried out in mirror confinement electron cyclotron resonance (MCECR) sputtering system [19] using a Langmuir single probe equipped with a designed simulated substrate as shown in Fig. 1. The microwave power operating at 2.45 GHz is supplied to the plasma chamber through a quartz window between the rectangular waveguide and the chamber. Two sets of magnetic coils and field yokes are used to generate a mirror confinement magnetic field, which can couple with the microwave to induce the cyclotron resonance movement of electrons. A round carbon target is set in the plasma chamber as solid carbon source for film deposition. During the plasma diagnosis process, the target is grounded and no bias voltage is applied in order to avoid severe sputtering on the target which might pollute the Langmuir probe. Argon as the plasma gas is inflated into plasma chamber through a gas inlet and the gas flux is controlled by mass flow meter. The single Langmuir probe with a tungsten tip of 0.2 mm in diameter is used to measure the floating voltage (V_f) of the argon plasma. The tip of the probe is located where the substrate is fixed during film deposition, as shown by the dash lined frame in the experimental apparatus labeled (a) and (b), where (a) stands for Langmuir probe and (b) stands for substrate holder, respectively. Concerning that the plasma condition near the substrate will be affected by the substrate bias voltage, a simulated substrate is designed to make the plasma condition near the Langmuir probe same as the actual deposition were in progress. The structure detail is shown in dash lined frame (a), in which a stainless steel plate is placed exactly where the substrate holder stays, and has the same size as the substrate holder, in addition to a hole in the center with the diameter of 10 mm, allowing the Langmuir probe to work normally. The simulated substrate is insulated from the plasma chamber and connected to a DC power supply which can apply a bias voltage (V_b). The plasma condition near the simulated substrate will be influenced by V_b, which leads to a change of saturation electron current (I_{e0}), so I_{e0} was recorded to investigate the effect of V_b on plasma diagnosis results. The Langmuir probe is connected to a signal analyzer to process the measurement automatically. Each measurement is repeated for 3 times and an average value is acquired.

2.2. Preparation of cross-linked GLEC and amorphous films

The preparation of carbon films are carried out in the experiment apparatus shown in Fig. 1, in which a substrate holder was set in the plasma chamber instead of Langmuir probe, as shown in dash lined frame (b). Carbon films were deposited on p-type Si (100) surface, using ECR plasma sputtering technique. Silicon wafer with the size of 20 mm × 20 mm × 0.6 mm was cleaned in acetone and ethanol bath successively by ultrasonic wave, then was fixed onto the substrate holder and put into the vacuum chamber. The vacuum chamber was pumped down to base vacuum of 3×10^{-4} Pa before argon was inflated to generate the ECR plasma. The working pressure was 4×10^{-2} Pa and the substrate surface was cleaned by Ar plasma for 3 min before a sputtering bias voltage of −300 V was applied onto carbon target. The bias voltage applying on the substrate varied from −50 V to +50 V in order to control the carbon film being deposited under either electron irradiation or ion irradiation, thus control the film structure to be either amorphous or cross-linked GLEC. The depositing time was 15 min and the substrate temperature rose from room temperature to less than 150 °C during the deposition process, which was measured by a thermal couple fixed behind the substrate holder. Table 1 showed the preparation details of carbon films.

2.3. Film characterization and tribotest

The binding configurations of carbon films were analyzed using X-ray photoelectron spectroscopy with a scan range from 0 to 1100 eV of binding energy. The film surfaces were cleaned by Ar ion before the analysis. The nanostructures of carbon films were observed using high resolution transmission electron microscopy with the electron acceleration voltage of 300 kV. Plan view HRTEM specimens were prepared by scraping the film from Si substrate and transferring

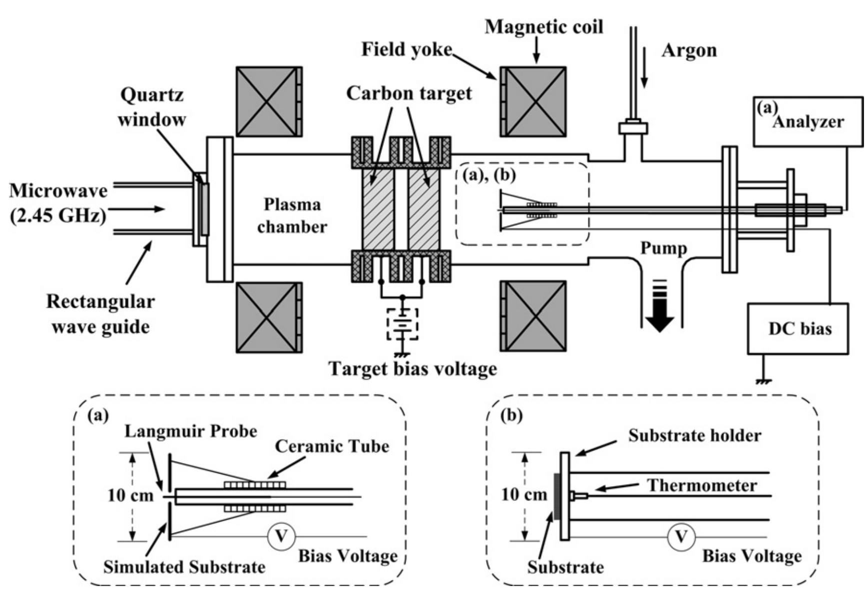

Fig. 1. Schematic illustration of the experimental apparatus.

Table 1
Preparation details of carbon films.

Sample number	Pressure (Pa)	Bias voltage (V)	Temperature rising (°C)
1	0.04	−10	34–72
2	0.04	+10	21–68
3	0.04	+50	29–131

the flakes onto copper micro grid. Cross-sectional specimens were prepared by mechanical polishing followed by ion beam thinning. The friction coefficients of amorphous and cross-linked GLEC films were tested on a pin-on-disk tribometer. The material of pin was Si_3N_4 ball (radius of 3.17 mm), the normal load was 2 N, the rotational speed was 180 rpm and the radius of wear track circle was 1.4 mm. The nanostructures of the wear tracks after tribotest were analyzed by HRTEM observation. The carbon films after tribotest were cleaned in acetone followed by carefully scratching on the wear track with a diamond pencil. The scrapings were then transferred onto copper micro grid for plan view HRTEM observation. This method has been widely used to prepare plan view TEM samples for nano crystallite carbon structure characterizing [2], and in this study the HRTEM results also proved that the scratching process didn't change the amorphous structure of carbon film, which will be shown in results section.

3. Experimental results

3.1. Plasma diagnosis results: I_{e0} and V_b

Fig. 2 showed I_{e0} as function of V_b at different pressures. It can be seen that I_{e0} at 0.01 Pa was much higher than at the other pressures, and as V_b rose up from −50 V to ±50 V, I_{e0} at each pressure increased evidently followed by a trend of decreasing. The figure also showed that the effect of bias voltage on I_{e0} was stronger at lower pressure, indicating that plasma condition near the substrate was steadier at higher pressure, which was favorable for high quality film preparation. Fig. 3 showed V_f as function of V_b at different pressures. It can be seen that V_f rose up slightly when V_b was under +30 V, and dropped rapidly as bias voltage rose up to +50 V, except the case of 0.01 Pa, where V_f monotonous rose up with V_b. The floating voltage also showed a dependence on gas pressure, in which V_f became higher as the gas pressure increased, except for the case of 0.01 Pa and 0.02 Pa when the bias voltage was lower than 0 V. This may be caused by measurement error in the plasma diagnosis and not considered in further discussion. It was known that once a substrate is placed into plasma, a sheath electric field was formed between the substrate surface and the plasma, and electrons or ions near the substrate were accelerated by the electric field to etch the substrate surface. The processes when electrons or ions etching the substrate surface were defined as electron irradiation or ion irradiation in this paper, respectively. The applied bias voltage on the substrate could generate another electric field, which overlaid on the sheath potential. When V_b and sheath potential was equal and opposite, the electric field would be neutralized, neither electron nor ion would be driven to the substrate surface, and this bias voltage value was called V_f. When V_b was higher than V_f, electrons would be driven to the substrate surface, and the film will grow under electron irradiation, otherwise under ion etching. So the irradiation mold could be easily controlled by changing substrate bias voltage. In Fig. 3, different irradiation molds responding to bias voltage at each pressure were divided by the diagonal line, on which bias voltage equals floating voltage. It was quite clear that as pressure increased, lower bias voltage was needed to achieve electron irradiation. The exception was in the pressure of 0.01 Pa, where electron irradiation couldn't be achieved in researched bias voltage range.

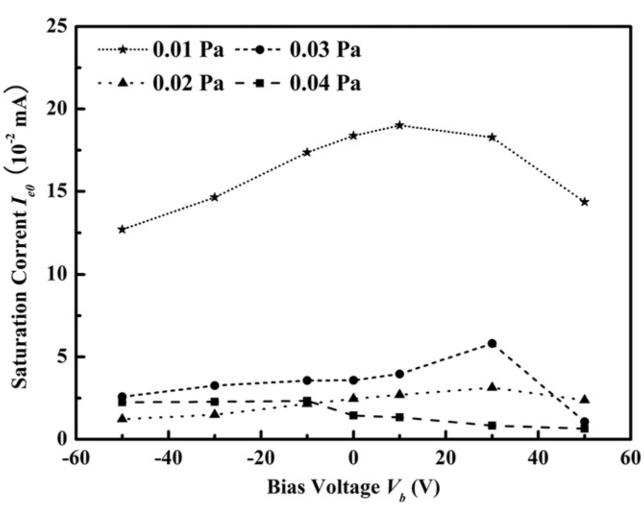

Fig. 2. I_{e0} as function of V_b at different pressures.

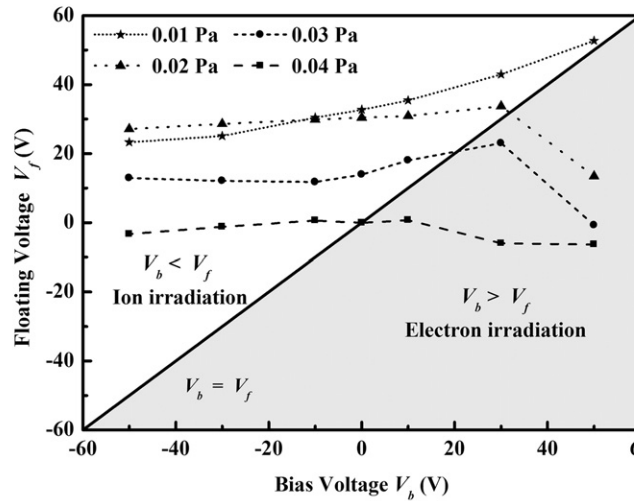

Fig. 3. V_f as function of V_b at different pressures.

3.2. Nano structure by using high resolution transmission electron microscopy

The nano-structural details of carbon films prepared using the bias voltage of −10 V, +10 V and +50 V were investigated by HRTEM images and Electron Diffraction patterns, and the results are summarized in Fig. 4(a), (b) and (c), respectively. Each figure contains a cross section view (left) and a plan view (right) HRTEM image and an ED pattern. In Fig. 4(a) the HRTEM images showed an amorphous structure, and the ED pattern has two diffraction rings with the diameter of 5.7 Å^{-1} and 8.7 Å^{-1}. In Fig. 4 (b) the film also showed amorphous structure and the ED pattern has two diffraction rings with the diameter of 3.2 Å^{-1} and 8.7 Å^{-1}.

In Fig. 4 (c), nano crystallite consisting of multi-graphene layers in the amorphous carbon matrix can be clearly seen in the plan view image, and there was also a single graphene sheet embedded in amorphous matrix, as indicated in the figure. The size of nano crystallite was between 1–5 nm, inside which graphene layers were distributed in bending or curving shape. ED pattern showed strong diffraction rings with the diameter of 2.8 Å^{-1}, 5.7 Å^{-1} and 8.7 Å^{-1}, and the homogenous lightness suggested that the nano crystallite were randomly distributed. The 2.8 Å^{-1} diffraction ring corresponded to interplanar spacing of 0.36 nm, which is close to interplanar spacing between graphene layers, indicating that the nano crystallite regions

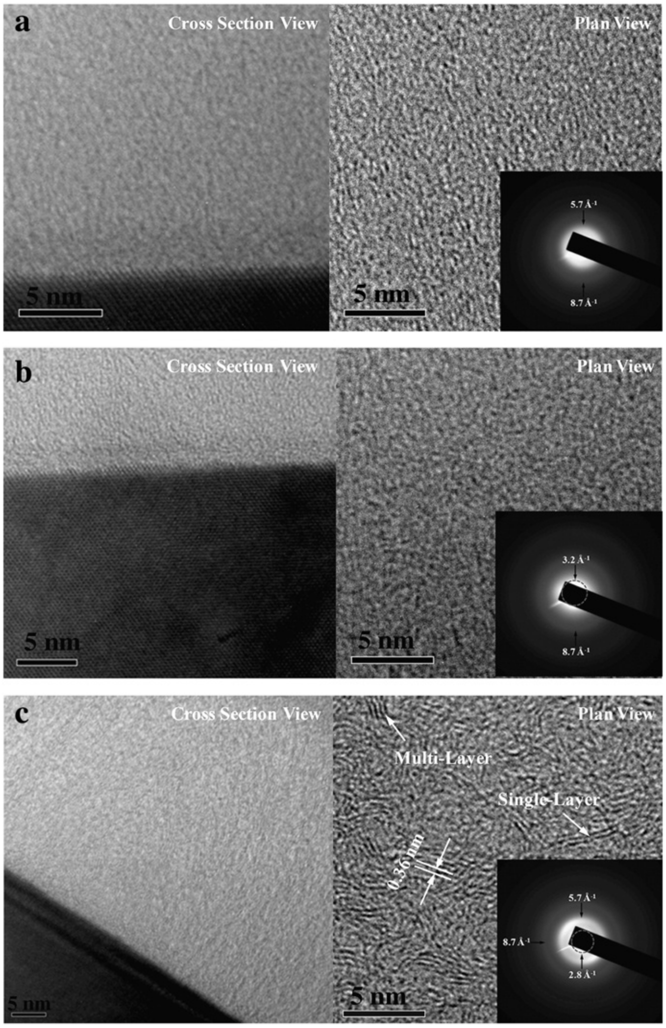

Fig. 4. HRTEM images and ED patterns of carbon films prepared with the bias voltage of (a) −10 V, (b) +10 V and (c) +50 V.

contain series of graphene sheets. This spacing was also marked in Plan view HRTEM image, which coincided with the ED results. From the cross section view, the graphene layers were found to aline normally to the Si substrate, indicating the graphene layers were formed in an oriented growth process. The graphene layers in the normal direction to substrate was tens of nanometers in length, and connected to each other at the distal ends with bending and buckling, composing longer crystallite graphene layers through the film thickness. The HRTEM results suggested that carbon film prepared using +50 V bias voltage had a nano crystallite structure, while the films prepared using −10 V and +10 V were amorphous.

3.3. Binding configuration by using X-ray photoelectron spectroscopy

Binding configurations of carbon films were acquired from XPS spectra. Fig. 5 shows XPS spectra of specimen prepared with bias voltage of +50 V, and the spectra of other two specimens were analyzed with the same method. As shown in Fig. 5, the original C-1s spectrum (gray dots) was decomposed into three Gaussian-distributing curves (green lines), composing a fitted spectrum (red line), and each curve indicated one carbon atom binding condition. The two main curves with the peak position at 284.4 eV and 285.2 eV indicated C=C bonds and C−C bonds, on which carbon atoms were sp^2 and sp^3 hybridized respectively. Another minor curve with the peak position at 288.8 eV indicated C−O bonds, which meant some carbon

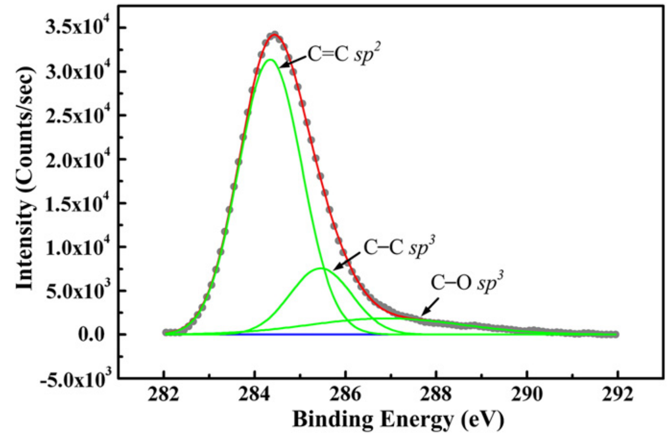

Fig. 5. Typical fitting results of the XPS spectrum, in which the gray dots are raw data, the green curve are decomposed curves and the red curve is the fitted spectrum. The sample was carbon film prepared with the bias voltage of +50 V.

atoms on the film surface were also bonded with oxygen atoms. The C−C binding and C=C binding were essential for realizing the binding configurations of carbon films. Fig. 6 showed the contents of sp^2 and sp^3 hybridized carbon atoms in the films as function of bias voltage. It was clear that as bias voltage rose from −10 V to +50 V, the sp^2 content increased from less than 50% to more than 70%, indicating that higher bias voltage resulted in higher sp^2 content.

3.4. Tribotest results

Fig. 7 shows the tribological curves of friction coefficient for amorphous carbon film and cross-linked GLEC film, which were obtained on a pin-on-disk tribometer. The amorphous carbon film used for tribotest was prepared using bias voltage of −10 V, and the cross-linked GLEC carbon film was prepared using bias voltage of +50 V, as those in Fig. 4(a) and (c). In Fig. 7 (a), it is clear that the friction coefficient of amorphous carbon film was 0.26 at the beginning of tribotest, and decreased to 0.073 after about 5000 cycles of sliding rotation. The wear life of the amorphous carbon film was more than 16,000 cycles, and the low friction stage was stable, indicating the amorphous carbon film is suitable for low frictional coating. In Fig. 7(b), it can be seen that the friction coefficient of the cross-linked GLEC film is

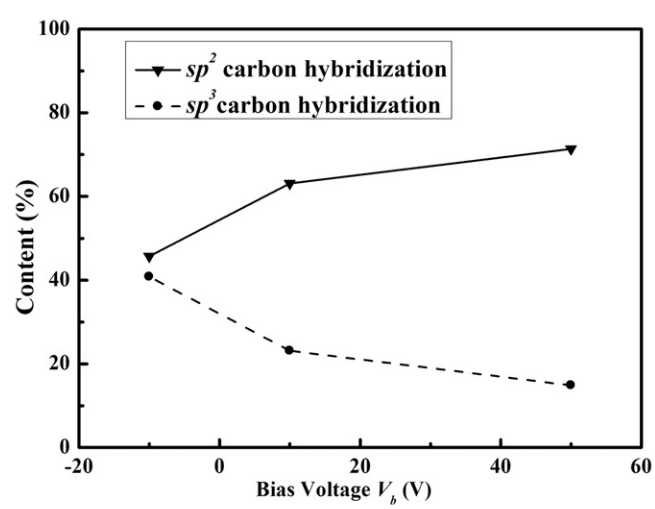

Fig. 6. Contents of *sp2* and *sp3* hybridized carbon atoms in carbon films with different bias voltage.

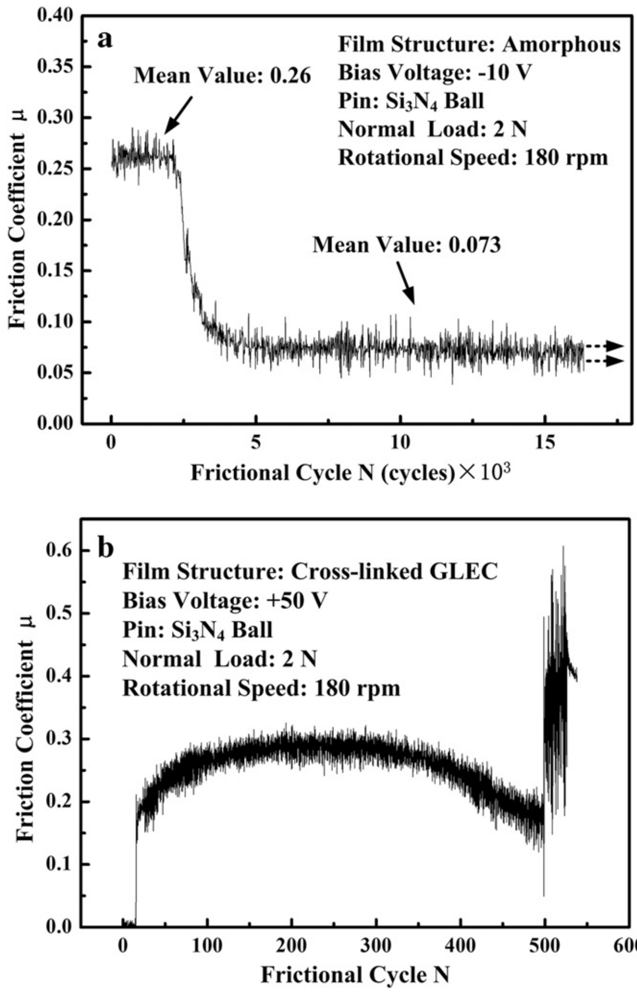

Fig. 7. Tribotest results of (a) amorphous carbon film prepared under bias voltage of −10 V and (b) cross-linked GLEC film prepared under bias voltage of +50 V.

between 0.2 and 0.3, and the friction coefficient of more than 0.5 after about 500 cycles represents the sliding wear of Si_3N_4 pin against silicon substrate, which is usually seen at the end of tribotest when the carbon film was destroyed. This short wear life could be caused by insufficiency adhesion between the carbon film and the Si substrate.

Fig. 8 showed the HRTEM images and ED pattern of the wear track of the two films, in which (a) showed the structure of amorphous carbon film at the low friction stage, and (b) showed the structure of cross-linked GLEC film, respectively. By comparing Fig. 8(a) with Fig. 4(a), it is clear that the amorphous structure of the carbon film changed into a local crystallized structure containing nano clusters of graphene layers, as marked for instance in Fig. 8(a). The ED pattern showed a diffraction ring with the diameter of 3 Å, corresponding to interplanar spacing of 0.33 nm, which was closed to that between graphite {002} planes. Concerning the low friction behavior of hydrogen free a-C film, there are two widely accepted explanations which are the formation of transfer film on counter sliding surface and the graphitization of transfer film, those were also studied in our earlier research. In this study, however, the structural change on the wear track of film surface was firstly observed by HRTEM, which provided direct evidence of graphitization of hydrogen-free amorphous carbon film in tribological action. This structural change from amorphous structure to nano crystallite structure with graphene layers can be one of the reasons why the friction coefficient decreased during friction contact, since graphite like structure can provide low friction coefficient in ambient environment.

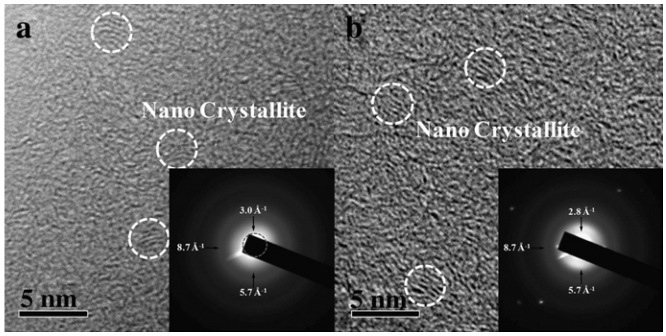

Fig. 8. HRTEM images and ED pattern of the wear track of (a) amorphous carbon film prepared under bias voltage of −10 V and (b) cross-linked GLEC film prepared under bias voltage of +50 V.

From Fig. 8(b), it can be seen that the wear track of cross-linked GLEC film slightly changed into less organized nanostructure than the original deposited film, though it remains nano crystalline structure. The ED pattern contains diffraction rings with the same diameter as that from as deposited GLEC film, in addition to [100] Si spots pattern. By comparing the HRTEM images of original surface and wear track of the amorphous carbon (see Fig. 4(a) and Fig. 8(a)) and cross-linked GLEC film (see Fig. 4(c) and Fig. 8(b)), it was found that both wear track and original surface of the cross-linked GLEC film showed the similar structure as the wear track of amorphous carbon film which was in stable low friction stage. Notably, the wear track of the amorphous carbon film at low friction stage after 15,000 cycles of sliding contact showed a quite similar nanostructure with the wear track of cross-linked GLEC film, which was obtained after only 500 cycles of sliding contact.

4. Discussion

The nanostructure of cross-linked GLEC film is apparently different from the amorphous carbon, and the only difference in film deposition was the substrate bias voltage, so it's convincible that bias voltage is the main cause of the film structure difference. The plasma diagnosis results showed that at the bias voltage of +50 V, when cross-linked GLEC film can be prepared, the film was deposited under electron irradiation, and the amorphous carbon film was prepared at the bias voltage of −10 V, when the film was deposited under ion irradiation. By comparing the deposition condition of the films with different nanostructure, a reasonable explanation can be suggested that the cross-linked graphene layer structure was formed in the assist of incidence electrons. This explanation is different from that in McKenzie, et al.'s work [4], where the formation of graphite-like structures was believed to be mainly contributed by high energy incidence carbon ions. The temperature rising during film deposition showed that the GLEC film was prepared under 150 °C, which was much lower than thermally induced graphite-like structure transition in tetrahedral amorphous carbon films in Orwa, et al.'s work [6], in which the amorphous structure did not change into a mainly graphite-like structure until 500 °C. So apparently the growing of graphene layers in ECR plasma sputtering relies on its specific plasma condition, which is electron irradiation as discussed above.

The growing mechanism of graphene nano crystallite under electron irradiation is an interesting topic. One possible mechanism is that the electron irradiation causes instantaneous high temperature, say more than 500 °C, at some local regions on substrate surface, where a phase change of amorphous carbon can be induced. However, the measured temperature is far below the phase change temperature. Considering thermal exchange and inhomogeneous distribution of surface temperature, the actual highest temperature on substrate surface will be higher than the average temperature measured in this study. However, instantaneous high temperature on certain region of substrate surface is hard to obtain, which is an important proof to confirm this mechanism, so further research should be carried out. The other possible mechanism is that the incident electrons may brake σ bonds between carbon atoms and induce π bonds forming. This mechanism should be taken into consideration, especially when the instantaneous temperature on substrate surface is not so high to cause phase change. The two above mechanisms worth more in-depth research in the future, because in any case, the growing mechanism of nano crystallite under electron irradiation is different from that under ion irradiation.

The identifying of electron irradiation in this study involved a modified Langmuir single probe, which has a large area electrode (the simulated substrate) near the probe tip. So the plasma condition near the probe tip is different from that far away in the uniform plasma. Also, the floating voltage obtained in this study is only suitable for the area near the probe tip, where the author believes plasma condition is decisive for film deposition. Because it is difficult to measure the actual movement of ions and electrons that fly to the substrate and irradiate the film, it is an approximate treatment to identify electron irradiation by measuring the plasma condition near the substrate. More precise and direct evidence should be given in further research to prove the electron irradiation on substrate.

By comparing the TEM images of amorphous carbon and cross-linked GLEC film and their wear tracks (see Fig. 4(c) and Fig. 8(a)), we found that the wear track of amorphous carbon film in low friction stage has the similar structure with as deposited cross-linked GLEC film. From the result of amorphous carbon film it can be seen that before the low friction stage, there is a high friction stage where the friction coefficient gradually decreased, which took about 2500 cycles of friction. This stage is not preferred when we consider the carbon film as a lubricant coating supplied for industrial field. Then it is necessary to shorten or even avoid the high friction stage. Since the cross-linked GLEC film has the similar structure with the low-friction-stage carbon film, and this structure can be obtained by electron irradiation in film deposition, then we found a way to prepare carbon film which has the potential to show low friction coefficient at an earlier stage of the friction. In Fig. 7(b), it should be noticed that the friction coefficient of cross-linked GLEC film showed a decreasing trend after 500 cycles of friction, which is one fifth of the cycles for amorphous carbon film. However, the interfacial strength between the film and the substrate was not enough to survive long period friction, so the spalling of the film happened before the low friction coefficient stage was observed. Nevertheless, it is an interesting way to improve the friction durability of the cross-linked GLEC film in the aim of providing a new kind of carbon film as lubricant coating which can show low friction as soon as the friction begins. We believe by adjusting parameters in deposition, the interfacial strength will be increased and the film structure will be more closed to which can achieve low friction at the beginning of the friction. Further research will be focused on these subjects and the results will be reported in the near future.

Considering the good electrical conductivity of graphene layer, the GLEC film may have special electrical property, which gives it more potential applications, such as a conductive lubricating film. Apparently, this study only investigated portion of the GLEC properties, which is the tribological property. More study is needed for further use of GLEC films.

5. Conclusion

In this paper, a new path to prepare cross-linked GLEC film introducing electron irradiation in ECR plasma sputtering was found. Cross-linked GLEC film has been prepared, and the graphene layers in the film were found to grow normally to the silicon substrate, and connect to each other with bending and buckling edges, forming a cross-linked structure embedded in amorphous matrix. The graphitization of hydrogen-free carbon film in tribological test was firstly observed by HRTEM, which gave strong evidence to explain the mechanism of friction coefficient decreasing of amorphous carbon film. The cross-linked GLEC film showed similar structure with the wear track of amorphous carbon which was in stable low friction stage, indicating that the cross-linked GLEC film has the potential to achieve low friction coefficient at the beginning of sliding contact.

Acknowledgment

The authors thank the National Nature Science Foundation of China with Grant Number of 90923027.

References

[1] I. Alexandrou, H.J. Scheibe, C.J. Kiely, A.J. Papworth, G.A.J. Amaratunga, B. Schultrich, Phys. Rev. B 60 (1999) 10903.
[2] S. Hirono, S. Umemura, M. Tomita, P. Kaneko, Appl. Phys. Lett. 80 (2002) 425.
[3] K. Matsuda, S. Hirono, H. Takayanagi, Physica B 329–333 (2003) 1529.
[4] D.W.M. Lau, D.G. McCulloch, M.B. Taylor, J.G. Patridge, D.R. Mckenzie, N.A. Marks, E.H.T. Teo, B.K. Tay, Phys. Rev. Lett. 100 (2008) 17601.
[5] D.W.M. Lau, A. Moaf, M.B. Taylor, J.G. Partridge, D.G. McCulloch, R.C. Powles, D.R. McKenzie, Carbon 47 (2009) 3263.
[6] J.O. Orwa, I. Andrienko, J.L. Peng, S. Prawer, Y.B. Zhang, S.P. Lau, J. Appl. Phys. 96 (2004) 6286.
[7] C. Donnet, A. Erdemir, Tribol. Lett. 17 (2004) 389.
[8] C. Donnet, T. Le Monge, L. Ponsonnet, M. Belin, A. Grill, V. Patel, C. Jahnes, Tribol. Lett. 4 (1998) 259.
[9] J. Fontaine, C. Donnet, A. Grill, T. Le Monge, Surf. Coat. Technol. 146–147 (2001) 286.
[10] J.C. Sanchez-Lopez, A. Erdemir, C. Donnet, T.C. Rojas, Surf. Coat. Technol. 163–164 (2003) 444.
[11] J. Fontaine, M. Belin, T. Le Monge, A. Grill, Tribol. Int. 37 (2004) 869.
[12] A. Erdemir, J. Fontaine, C. Donnet, Tribology of diamond-like carbon films: fundamentals and applications: An overview of superlubricity in diamond-like carbon films, 2008, p. 237.
[13] H. Ronkainen, K. Holmberg, Tribology of diamond-like carbon films: fundamentals and applications: Environmental and thermal effects on the tribological performance of DLC coatings, 2008, p. 155.
[14] T.W. Scharf, I.L. Singer, Tribol. Lett. 36 (2009) 43.
[15] Y. Liu, A. Erdemir, E.I. Meletis, Surf. Coat. Technol. 82 (1996) 48.
[16] Y. Liu, A. Erdemir, E.I. Meletis, Surf. Coat. Technol. 86–87 (1996) 564.
[17] Y. Liu, A. Erdemir, E.I. Meletis, Surf. Coat. Technol. 94–95 (1997) 463.
[18] K.Y. Li, Z.F. Zhou, I. Bello, C.S. Lee, S.T. Lee, Wear 258 (2005) 1577.
[19] C. Cai, D.F. Diao, W. Ma, Y. Yan, Vacuum 80 (2006) 939.